

Scene Recognition with Objectness, Attribute and Category Learning

Ji Zhang, *Fellow, IEEE*, Jean-Paul Aïnam, *Member, IEEE*, Li-hui Zhao, Wenai Song, and Xin Wang

Abstract—Scene classification has established itself as a challenging research problem. Compared to images of individual objects, scene images could be much more semantically complex and abstract. Their difference mainly lies in the level of granularity of recognition. Yet, image recognition serves as a key pillar for the good performance of scene recognition as the knowledge attained from object images can be used for accurate recognition of scenes. The existing scene recognition methods only take the category label of the scene into consideration. However, we find that the contextual information that contains detailed local descriptions are also beneficial in allowing the scene recognition model to be more discriminative. In this paper, we aim to improve scene recognition using attribute and category label information encoded in objects. Based on the complementarity of attribute and category labels, we propose a Multi-task Attribute-Scene Recognition (MASR) network which learns a category embedding and at the same time predicts scene attributes. Attribute acquisition and object annotation are tedious and time consuming tasks. We tackle the problem by proposing a partially supervised annotation strategy in which human intervention is significantly reduced. The strategy provides a much more cost-effective solution to real world scenarios, and requires considerably less annotation efforts. Moreover, we re-weight the attribute predictions considering the level of importance indicated by the object detected scores. Using the proposed method, we efficiently annotate attribute labels for four large-scale datasets, and systematically investigate how scene and attribute recognition benefit from each other. The experimental results demonstrate that MASR learns a more discriminative representation and achieves competitive recognition performance compared to the state-of-the-art methods.

Index Terms—Scene classification, object detection, attribute recognition, attribute annotation.

I. INTRODUCTION

SCENE recognition, a.k.a, scene categorization, aims to determine the overall scene category (e.g., beach, kitchen, airport) by laying an emphasis on understanding its global properties [1], [2]. It is a high-level computer vision task that allows definition of context for object recognition. Whereas tremendous progress in object detection and semantic segmentation tasks has been achieved [3], [4], the performance at scene recognition has not attained the same level of success [1], [5]. Despite the increasing attention given by researchers to solve the scene recognition problem, it still remains a challenging task.

Early attempts at recognizing high-level scene properties used hand-engineered features [6]. For instance, Xiao et al.[6]

Ji Zhang, J.-P Aïnam, W. Song are with the School School of Software, North University of China, Taiyuan, China

X. Wang is with Southwest Petroleum University, China.

W. Song is with Shanxi Research Center of Software Engineering Technology, Taiyuan, China

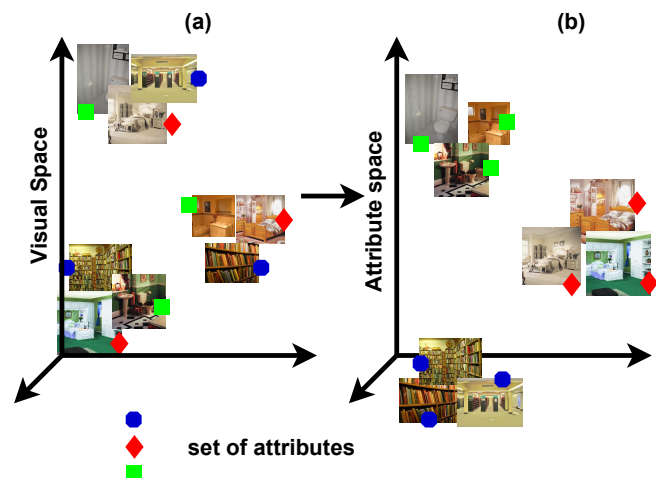


Fig. 1: Motivation: using visual feature alone, it’s difficult to discriminate visually similar images. On the other hand, attributes are semantically descriptive across classes.

investigated the benefits of several well-known low-level descriptors such as HOG [7], SIFT [8], and SSIM [9] while Meng et al.[10] proposed a global image representation using Local Difference Binary Pattern (LDBP). These methods can learn sophisticated features to describe the visual appearance of scenes. However, they rely heavily on specific types of visual cue, such as color, texture, or shape, which are not practical and powerful enough to discriminate scenes with similar visual appearances.

Current techniques for assigning semantic label to scenes are mostly based on Convolutional Neural Networks (CNNs) [11], [12], [13]. Specifically, Donahue et al.[12] investigated the semantic clustering of deep convolutional features, and Xie et al.[13] proposed to combine CNN features with dictionary-based models. These methods only use the image features to recognize the scene and fail to produce robust scene representations. Other recent works consider semantic information about object attributes and states. For example, Chen et al.[14] adopted a contextual-based model for discovering regions in scene images using spatial structural layouts and Alejandro et al.[3] used semantic segmentation as an additional modality of information for scene recognition.

In general, context information such as semantic segmentation, structural layouts and object attributes have become the key to improve scene recognition accuracy. In particular, semantic attributes are used to enable a richer description of scenes while semantic segmentation enables spatial relation-

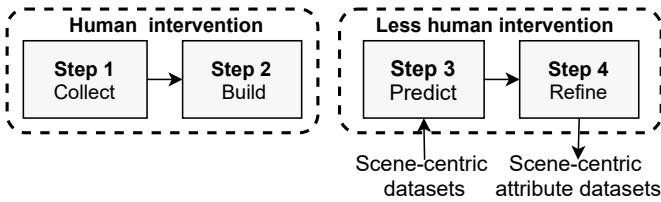


Fig. 2: The four steps of our annotation strategy. We create a new set of object attributes for a scene dataset using predicted objects from object detection models.

ships between objects in a scene. As shown in Figure 1, it is difficult to distinguish the three categories using only visual features, while on the attribute space, it’s easier to semantically differentiate the images across categories. Attribute information are quite important to discriminate similar images and boost the performance of scene recognition. However, extracting object attributes or building an effective semantic representation have proven to be quite challenging, especially when the object attribute annotation must be made through human effort. Semantic segmentation is also challenging given that the task of labeling a scene with accurate per-pixel labels is time consuming.

To overcome the above limitations, we first propose a partially supervised annotation strategy in which human supervision and intervention are reduced and are only required on few tasks. The strategy is flexible and provides a much more cost-effective solution to real world scenarios, and requires much less annotation efforts. An overview of the annotation approach is depicted in Figure 2. We begin by identifying pre-trained models for the task of object detection. Then, we use these models to predict object instances for the scene images. Since image scenes are composed of objects, we can use object predictions as attributes to describe scenes. However, this simple, yet effective approach has a major drawback in that attribute predictions are not always highly reliable due to possible biases on their training data. We solve this problem by only keeping those attributes with high confidence scores while discarding those attributes with low confidence scores. In addition, we include these attributes into our model through a regularized loss specifically adapted for this purpose. Moreover, Zamir et al.[15] showed that scene recognition, object detection and semantic segmentation are interrelated tasks that share a common Branch and that, under transfer learning setting, the performance of object detection methods is generally higher than that of scene recognition. As a result, objects predictions mined from scene images using object detection models can also benefit the scene recognition task.

Following the strategy above, we exploit both local (attribute features) and global information (image features) to learn a better scene representation. We use the detected score to control the importance of each attribute while previous works based on attributes do not consider their importance. Many attributes usually co-occur for a scene with a different level of importance, and these scores may be helpful. For example, the object “table”, “computer” and “chair” better describe the scene category ‘office’ than the object “suitcase”. Given these

objects in a scene, the contributions of “table”, “computer” and “chair” must be considered. Motivated by this, we therefore introduce a Re-weighting Attribute Layer that utilizes the confidence scores of object in the scene to optimize scene recognition.

Compared with previous methods, our work differs in two aspects. First, we propose to investigate object information from object-centric datasets as attribute labels to the task of scene recognition. These attribute labels provide detailed local descriptions. Secondly, we propose a Multi-task Attribute-Scene Recognition (MASR) network that exploits attribute information in terms of objects scores to improve the scene recognition task. Various object and context information learned from object detection models are utilized as attributes. Moreover, we categorize the list of attributes into the probable and significant ones based on their prediction effectiveness and introduce a layer which adaptively incorporates the attribute into the network.

Our contributions are summarized as follows:

- 1) We propose an attribute mining strategy and release a set of scene attributes for MIT67 [16], SUN397 [6], ADE20K [5] and Places-365 [17] datasets. Code and attribute annotations for the datasets will be made publicly available after the blind-review process is completed.
- 2) We propose a novel multi-task attribute-scene recognition framework. The framework learns discriminative CNN embeddings for both scene recognition and attribute recognition.
- 3) We introduce an attribute re-weighting layer which leverage the attribute predictions to correct the classification based on the detected scores.
- 4) We achieve very competitive results for our proposed the method compared with the state-of-the-art scene recognition methods on four large-scale datasets.

The remainder of this paper is organized as follows. In Section II, we present the related research work. Then, in Section III, we describe our attribute annotation strategy. In Section IV, we provide details of the proposed scene recognition model. In Section V, we present our experimental results on scene recognition task. Finally, we conclude this paper and discuss the future works in Section VI.

II. RELATED WORKS

In this section, we describe the existing works that are relevant to our approach. We start by presenting works for solving the scene recognition problem in general, then we elaborate on multi-modal approaches and, finally, we present the recognition models that make use of contextual information.

A. Scene recognition

Research for scene recognition can be roughly divided into two groups: those based on handcrafted feature representations and those based on deep machine learning. The first group of works focus on designing appropriate local descriptors for scenes and the second group uses CNN to learn scene embeddings.

Hand engineered descriptors such as SIFT [8], HOG [7] have been the fundamental component for computer vision tasks, including scene recognition. Bag-of-features (e.g. VLAD, Fisher kernel) have also shown great success on scene recognition. Laurent et al.[18] proposed to design a holistic low-level features using Generalized Search Trees (GIST) descriptor. Other works have combined local features from local patches with holistic features. For example, Lazebnik et al.[19] proposed a technique that partitions the image into fine sub-regions and computes histograms of local features for each sub-region. The resulting spatial pyramid is simply an efficient extension of an orderless bag-of-features image representation. Similarly, Krapac et al.[20] introduced an extension of bag-of-words image representations and Fisher kernels to encode both the spatial layout and the appearance of local features. In addition, Wu et al.[21] proposed CENsus TRansform hISTogram (CENTRIST), a visual descriptor for scene categorization that encodes the local structural properties within an image and suppresses detailed textual information. However, CENTRIST is not invariant to rotations and only utilizes the gray-scale information of images, which limits its application. Furthermore, Margolin et al.[22] proposed the Oriented Texture Curves (OTC) descriptor to capture the texture of a path along multiple orientation using the shapes of multiple curves, the gradients and curvatures, and the local contrast differences. In general, these handcrafted methods have failed as they depend on certain types of visual cue (e.g. color, texture, or shape) that are insufficient to distinguish between similar scenes. In addition, due to the handcraft nature of the features, these methods suffer a huge data bias without the flexibility on new datasets.

The second group of methods based on CNN usually result in better performance. Many works combine orderless bag-of-features or dictionary with CNN features to incorporate discriminative local and structural information. In particular, Cimpoi et al.[11] used a texture descriptor obtained by Fisher Vector pooling of a CNN filter bank and Xie et al.[13] combined features extracted from CNN with two dictionary-based representations. However, because of to the huge inter-class similarity in scene images, these approaches do not produce scene representations that are robust. To overcome this problem, recent techniques are based on multi-modality approach that incorporates context, attribute and object information into CNN to constrain scene recognition.

B. Hybrid and Multi-Modal architectures

In recent years, researchers have investigated how to effectively integrate local semantics of both objects and concepts in scene classification. In particular, Shuqiang et al.[23] proposed to combine a local feature codebook generated from both ImageNet and Places-365 datasets with the original features from scene images. Generally, hybrid-based methods first extract the local representations from image patches, and then aggregate their local representation by encoding methods. For example, Gong et al.[24] proposed a multi-scale orderless approach that performs orderless VLAD pooling on CNN activations at each level separately, and concatenates the resulting local

representations. Yang et al.[25] explored multi-scale CNNs by extracting features from multiple layers. Similarly, Cheng et al.[26] proposed a semantic descriptor where correlation of object configurations across scenes are exploited. ImageNet-CNN output score at the softmax layer is used to compute multinomial distribution using Bayes rule. However, Zhou et al.[2] showed that incorporating ImageNet features do not help much and demonstrated that object-centric and scene-centric neural networks differ in their internal representations. As a result, Zhou et al.proposed to learn from massive amounts of data by introducing a new benchmark with millions of labeled images. Similarly, Herranz et al.[27] presented an alternative method of combining features from an object-centric dataset that uses different scale ranges. Herranz et al.mainly addressed the scale induced dataset bias in multi-scale CNN architecture and showed an effectively way of combining scene-centric and object-centric knowledge (i.e., Places and ImageNet) in CNNs. However, the recognition accuracy highly depends on the scale, and carefully chosen multi-scale combinations are required to push the state-of-the-art recognition.

Recently, Yang et al.[28] proposed a dictionary learning layer composed of a finite number of recurrent units to simultaneously enhance the sparse representation and discriminative abilities of features. Pei et al.[29] used a mixed CNN-LSTM network that combines both visual and linguistic features like image captions. Furthermore, Alejandro et al.[3] exploited the spatial relationship between objects using both RGB images and semantic segmentation. However, as shown by the study of *taskonomies* [15], the performance of semantic segmentation methods is generally lower than that of object detection approaches. Thus, in this paper, we propose to enhance scene recognition using context information mined from object detection models.

C. Attributes for Image Recognition

The use of complementary information such as attributes has been proposed in several computer vision tasks including pedestrian recognition [30], [31], action recognition [32], [33], image recognition [34], [35], and scene recognition [36], [37].

In pedestrian recognition, Lin et al.[30] proposed a multi-task network which learns an identity embedding and at the same time predicts pedestrian attributes. Tay et al.[31] also proposed an Attribute Attention Network (AANet) that integrates person attributes and attribute attention maps into a unified framework. The effectiveness of attributes has also been studied in action recognition. In particular, Rueda et al.[38] introduced a search for attributes that represents signal segments for recognizing human activities while Yao et al.[32] combined attributes and parts. Here, the attributes are represented as verbs describing human actions, and parts are composed of objects related to the actions. Recently, Roy et al.[33] used local spatio-temporal features to capture the action attributes in a Gaussian mixture model.

In image recognition, basic attributes such as texture, shape and color have been extensively investigated in early works [34], [35]. In particular, Ferrari et al.[34] showed for the first time that attributes can be learned for object recognition

through weakly supervised learning and trained a set of classifiers to predict the existence of human-labeled attributes in the data. Both Lampert et al.[35] and Xian et al.[39] proposed transfer learning and zero-shot learning approaches respectively on the Animals with Attributes datasets (AwA and AwA2) [39], [35]. The two datasets contain 50 classes and 85 attributes with no image overlap.

In scene recognition, there exists only few works about attributes. For instance, Oliva et al.[40] proposed a small-scale scene dataset with 8 attributes describing the spatial structure of a scene (e.g., naturalness, openness, roughness etc.) and Wang et al.[41] created an outdoor scene dataset with 47 attributes. In addition, Patterson et al.[37] introduced a subset of the SUN dataset [6] containing 14,340 images annotated with 102 attributes and used the attributes as mid-level semantic information for scene recognition. Recently, Zeng et al.[36] proposed to aggregate more complementary visual features of the scene using features from the Attribute-ImageNet [42] and the Places [2] datasets.

In contrast to existing methods using attributes in general [34], [35], [33], [39], [36], and scene attributes in particular [40], [37], we do not manually annotate the attributes and we do not directly learn a weight for each attribute to control the attribute’s impact, but we leverage object detected score information contained in the attributes. By so doing, the model could use more of its parameters for learning to compensate in failure cases. Moreover, we go beyond the simple use of objects in scene recognition and propose to utilize existing object-centric datasets to bridge the gap between object recognition and scene recognition.

III. ATTRIBUTE ANNOTATION STRATEGY

Most datasets for scene recognition [1], [5], [6], [16], [17] provide labels that rarely fill the gap between scene classification and semantic scene description. Recently, an effort is made to provide not only category labels to scene, but also attribute labels for describing the objects within the scene [37], [40], [41]. However, the intensive human labor required to annotate such datasets limits its application, especially when the attribute distribution is large. In this paper, we propose to mine object and context information using object detection models. In particular, we start by collecting object attributes and context information from two popular object-centric datasets, namely COCO Object and COCO Panoptic, and then use the attributes for scene classification after discarding the less discriminative ones. COCO Object is an object-centric dataset that provides label to 80 different objects (i.e., *things*) while COCO Panoptic is an instance segmentation task addressing both *stuff* and *thing* classes. Here, *things* are countable objects (e.g., people, animals etc.) whereas *stuff* are regions of similar texture or material (e.g., sky, grass, road etc.). *Stuff* and *thing* classes are usually addressed independently and included separately to boost scene recognition [3], [26]. In this paper, we use both *stuff* and *thing* with scene categories in a unified framework. Table I presents some class instances for *stuff* and *thing*.

Our annotation strategy can be formalized as follow. Let S and T , be the set of *stuff* and *thing*, respectively. F_s and

TABLE I: Examples of stuff and thing classes from COCO Object and COCO Panoptic datasets.

Groups	Attributes
<i>Things</i>	bottle, cup, apple, sheep, dog, suitcase, tv, toilet...
<i>Stuff</i>	sea, river, road, sand, snow, wall, window, wall...

TABLE II: Some scene categories with the total number of attributes (#Att), the number of attributes discarded using Equations 3, 4 and the number of attributes used (#Used) for the MIT67 dataset.

Categories	#Att	# Eq. 3	# Eq. 4	#Used
airport_inside	51	12	39	6
cloister	31	8	23	5
computerroom	48	12	36	8
dining_room	43	7	36	9
fastfood_restaurant	63	16	47	7
waitingroom	37	8	29	6
office	49	8	41	9
bathroom	45	14	31	10

F_t , two pre-trained CNN models for the respective tasks. We denote by $\{x_1, x_2, \dots, x_n\} \in X$ a scene-centric dataset with only category labels. Our goal is to use F_s and F_t on X to predict distributions over S and T such that,

$$p_s = F_s(X) \quad \text{and} \quad p_t = F_t(X) \quad (1)$$

where $p_s \in \mathbb{R}^{|S|}$ and $p_t \in \mathbb{R}^{|T|}$ are the probability predictions over S and T , respectively. Given X , the final *stuff* + *thing* predictions $\mathcal{P} \in \mathbb{R}^{|S|+|T|}$, on the given scene dataset is defined as

$$\mathcal{P} = p_s \cup p_t \quad (2)$$

Note that, \mathcal{P} does not add to 1 and does not represent a probability distribution. A common method of consolidating the two probability distributions p_s and p_t is to simply average them for every set of values V , s.t. $\mathcal{P}(V) = \frac{p_s(V)+p_t(V)}{2}$, $\forall V \in S \cap T$. However, here, S and T do not always overlap and usually describe different data sources. Consequently, we simply merge p_s and p_t and use the object detection score as a confidence score.

A. Filtering less discriminative attributes

Generally, scene categories such as ‘airport-inside’ and ‘offices’ contain slightly more objects than other places (See Table II). This prior knowledge - also inferred from Figure 3) - can lead to a common problem in most scene recognition methods that use objects as a clue. When there is too much information such as attributes and relationships about the objects, it may be challenging to identify the category of the place correctly. Since our strategy selects several information from object-related tasks, it can not guarantee that all of the selected objects are helpful for scene recognition. To overcome this problem, we propose to further select elements of S and T based on their frequencies and detection scores.

Based on the detection scores: The object instances with detection score less than a threshold are discarded. Only objects with scores higher than a threshold are selected as scene attributes. We think that narrowing the scene description

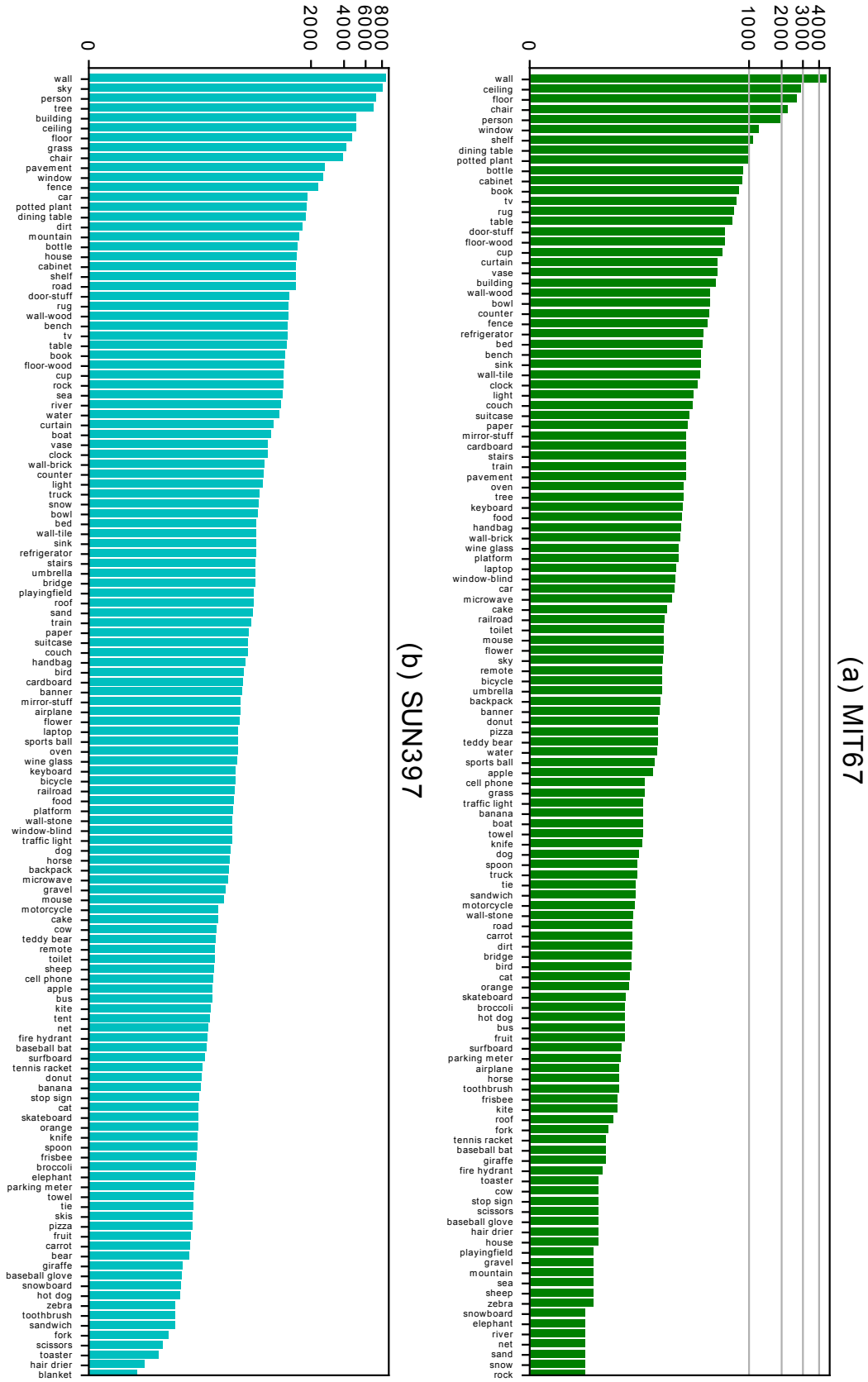


Fig. 3: Attribute distribution sorted by frequency on MIT67 and SUN397 datasets. (Zoom in for best view).

to the list of probable objects is much more realistic than using all the detections. We redefine \mathcal{P} as :

$$\mathcal{P}^* = \left\{ p_i \right\}_{i=1}^{|\mathcal{P}|} \mid p_i \in \mathcal{P} \text{ and } p_i > \xi \quad (3)$$

where ξ is the threshold. When the detection score is 0, the object is considered not present in the scene.

Based on the object frequency: We further consider attribute frequencies given a scene category and remove less common objects. For each category c , we define a relative attribute frequency as the number of non-zero score covering the category images. If $\{a^1, a^2, \dots, a^m\} \in \mathcal{A}_c$ is the set of detected attributes for c , an optimal \mathcal{A}_c^* is defined as

$$\mathcal{A}_c^* = \{a^j, \text{ s.t. } f_c(a^j) \geq \beta\}_{j=1}^m \quad (4)$$

where $f_c(a^j)$ is the relative frequency of attribute with the value a^j given the category c , β is the minimum frequency and $\mathcal{A}_c^* \in \mathbb{R}^{1 \times m}$ is the final list of attributes for c . As shown in Table II, using Equations 3 and 4 we can be sure to choose only representative objects to describe a category.

B. Comparison and dataset statistics

Many existing attribute datasets used ‘yes/no’ (or 0/1) to indicate whether the attribute is present or absent in the image [30], [43]. Even though this worked well and achieved some improvement in scene recognition task, it does not reflect how the humans often describe scene. Instead, in this paper, we use the detected score associated with the objects occurring in the image, mimicking a more natural object occurrence in daily scene. Moreover, the detected set of attributes can be easily and continuously enlarged as object detector models get more robust and efforts are made to annotate large object-centric datasets. A scene image is finally represented as a bag of attributes with their respective confidence scores. In Table III, we show some detected objects with their scores.

For both MIT67 and SUN397 datasets, we illustrate the attribute distributions in Figure 3. Figure 4a) shows the number of detected scores per samples. On average, each image is described by 6.5 objects present in the scene. Figure 4b) shows the distribution of the detection scores for 125 different objects. The maximum, average and minimum scores are illustrated. This shows that more than 50% of the objects can describe a scene with a maximum score of 100% and less than 25% produced a minimum score of 50%. On average, 70% to 80% objects from \mathcal{S} and \mathcal{T} are detected on the MIT67 dataset.

The proposed strategy can be generalized to N tasks that share a common Branch with scene recognition task. Equation 2 can then be formulated as:

$$\mathcal{P} = p_1 \cup p_2 \cup \dots \cup p_N \quad (5)$$

where $p_i = F_i(X)$, F_i a pre-trained CNN model for a task i . \mathcal{P}^* and \mathcal{A}_c^* are similarly obtained using Equations 3 and 4. In the next section, we present a method that leverages the scene category and our annotation to improve scene recognition task.

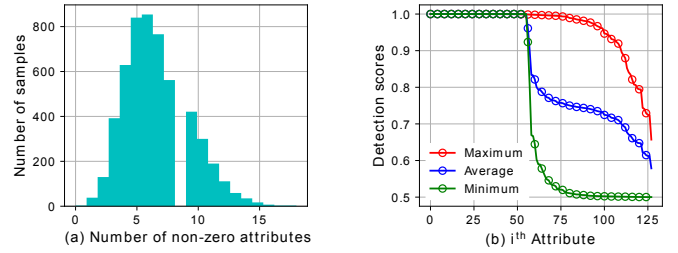


Fig. 4: Statistics from MIT67 dataset. (a) The histogram of samples per predictions. (b) The maximum, average and minimum detection scores for 125 objects.

IV. THE PROPOSED METHOD

We start by describing two baselines in Section IV-A, and then introduce our proposed Multi-task Attribute-Scene Recognition network in Section IV-B.

A. Baselines

Let $\mathcal{X}_I = \{(x_1, y_1) \dots, (x_n, y_n)\}$ be the set of scene images, where x_i denotes the i -th image and y_i its corresponding category. For each image x_i , we have a set of attribute annotations $\mathbf{a}_i \in \mathbb{R}^{1 \times m} \mid \mathbf{a}_i = \{a_i^1, a_i^2, \dots, a_i^m\}$ where a_i^j is the j -th attribute label for the image x_i , and m is the number of attribute labels. Let $\mathcal{X}_A = \{(x_1, a_1), \dots, (x_n, a_n)\}$ be the set of attributes. Note that, \mathcal{X}_I and \mathcal{X}_A share common scene images $\{x_i\}$. Based on \mathcal{X}_I and \mathcal{X}_A , we define two baselines:

Baseline 1: Scene classification baseline. Similar to [3], we take different backbones (e.g. ResNet, VGGNet, etc.), from which we modify the classifier layer to match the number of category K . Using only \mathcal{X}_I , this baseline considers scene recognition training process as an image classification task and defines an objective function such that:

$$\min_{\theta_I, w_I} \sum_{i=1}^n \ell(f_I(w_I, \phi(\theta_I, x_i)), y_i) \quad (6)$$

where ϕ is the backbone model parameterized by θ_I to extract features from the input image x_i , f_I is the classifier layer parameterized by w_I , which classifies the feature embeddings $\phi(\theta_I, x_i)$ into K -dimensional vectors representing the scene categories. ℓ is the cross-entropy loss.

Baseline 2: Scene attribute baseline. This baseline uses the attribute data \mathcal{X}_A and predicts the scene attributes. The model is trained using the following objective function:

$$\min_{\theta_A, w_A} \sum_{i=1}^n \sum_{j=1}^m \ell(f_{A_j}(w_{A_j}, \phi(\theta_A, x_i)), a_i^j) \quad (7)$$

where f_{A_j} is the j -th attribute classifier, parameterized by w_{A_j} , to predict the m attributes using the embedding $\phi(\theta_A, x_i)$. We take the sum of all the losses for m attribute predictions on the input image x_i as the loss.

For the evaluation of the classification baseline, we use Top@k accuracy metric with $k \in [1, K]$. Top@k measures the percentage of testing data whose topk-scored class coincides with the ground-truth label. To evaluate the attribute baseline,

TABLE III: Samples from Detectron2 model [4]. We only show objects with more than 80% precision. Images come from MIT67 and SUN397 datasets. (Zoom in for best view)

bathroom



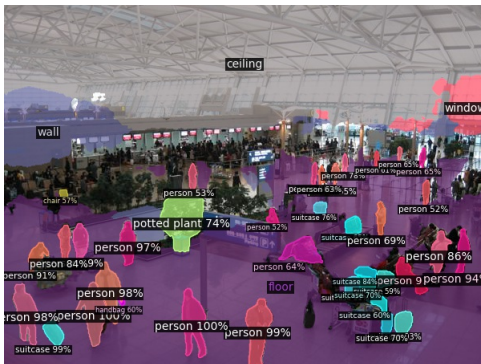
mirror-stuff
window
toilet
floor
sink 100%

fastfood



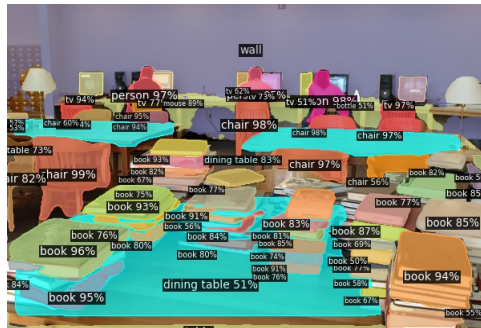
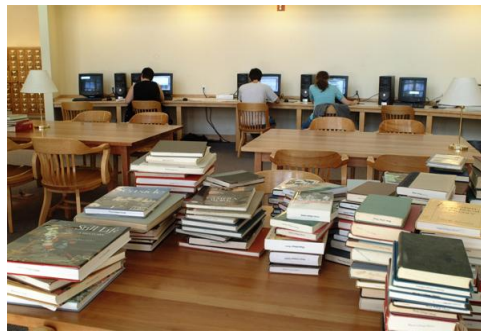
ceiling
wall
window
chair 98%
dining table

airport



ceiling
wall
window
person 99%
suitcase 99%

library



wall
book 97%
person 97%
chair 97%
tv 94%

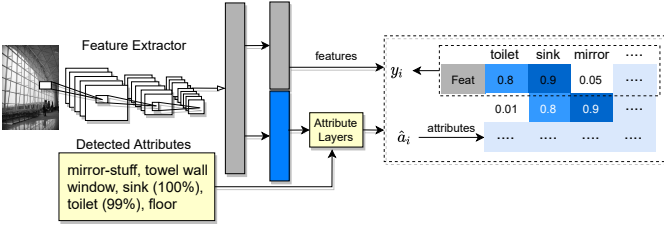


Fig. 5: Overview of the MASR architecture. The attribute information are obtained from pre-trained object-centric models. Attributes are used to support the learning of the CNN feature through a regularized loss and a re-weighting layer. The re-weighting layer enforces weights for attributes and reduce the influence of unreliable attributes on the scene result.

we take the classifier layer output and evaluate it with the ground-truth using the classification metric.

B. Multi-task attribute-scene architecture

In this section, we aim to improve scene recognition task using complementary cues from attribute labels. It has been established that scene attributes may contain information which is often highly relevant to the scene recognition task. However, different from existing works, this paper leverages automatically generated attributes with a varying degree of scores. The idea is to add a simple, yet effective attribute scores to the category level features such that the attribute information is able to drive the learning procedure. The overview of the proposed approach is illustrated in Figure 5. The network contains two parts. The first part predicts the scene category label, and the second part predicts the attribute labels. Given a scene image x_i , we first extract its feature representation $\mathbf{v}_i = \phi(\theta_I, x_i)$, using a CNN-like network. Secondly, we take attribute scores as additional cues and re-weight \mathbf{v}_i . Then the resulting features is passed through a fully connected layer $L^{|K|}$ for predictions. Simultaneously, we use \mathbf{v}_i to predict the attribute probabilities p_{att} using a fully connected layer $L^{|A|}$, where A is the set detected attributes.

Attribute task loss. Since our attributes are not completely mutually exclusive, the prediction of multi-attribute is a multi-label classification problem. The structure of the layer that predicts the attributes is different from the traditional single-label classification layer that includes one cost function. In order to predict all attributes, we employ a multi-class cross entropy loss defined as:

$$\mathcal{L}_{att} = -\frac{1}{n} \sum_{i=1}^n \sum_{j=1}^m \left(\hat{a}_i^j \log(p_{att}(x_i, a_i^j)) + (1 - \hat{a}_i^j) \log(1 - p_{att}(x_i, a_i^j)) \right) \quad (8)$$

where $p_{att}(x_i, j)$ is the predicted class probability on the j -th attribute of the training sample x_i , and $\hat{a}_i^j \in \{0, 1\}$ is the attribute ground-truth defined as:

$$\hat{a}_i^j = \begin{cases} 1 & \text{if } a_i^j > \xi \\ 0 & \text{otherwise} \end{cases} \quad (9)$$

The loss in Equation 8 usually suffers from imbalances in the training data. Some objects such as “person” are much more frequent than others (see Figure 3), and we cannot simply compensate by data sampling, because attributes co-occur and balancing the occurrence frequency of one attribute will change that of others. To address this, we introduce a regularizer β^j which reflects the relative frequency of j -th attribute in the training data (i.e., its ratio of positive to negative attribute labels). Equation 8 then becomes:

$$\mathcal{L}_{att} = -\frac{1}{n} \sum_{i=1}^n \sum_{j=1}^m \left(\hat{a}_i^j (1 - \hat{a}_i^j) \cdot \beta_k^j \cdot \log(1 - p_{att}(x_i, a_i^j)) \right), \quad \beta_k^j = \frac{\|a_k^j\|}{\sum_{l=1}^K \|a_l^j\|_{l \neq k}} \quad (10)$$

where $\|a_k^j\|$ is the number of samples holding the k -th class label of the j -th attribute (i.e., the magnitude of the j -th attribute for the k -th scene category). Note that, the classifiers for different attribute features are not shared.

Attribute Layers. Because the attribute representation is learned on separate data, we can expect some of the attributes to be much important than others. We thus introduce a layer that re-weight the attributes using the detected scores. It is composed of some linear transformations that aggregate all attribute information into a single vector \mathbf{v}_i . We denote by $\tilde{\mathbf{a}}_i = p_{att}(x_i, \mathbf{a}_i) \in \mathbb{R}^{1 \times m}$ the attribute scores from the attribute classifier f_A . We then learn the confidence score \mathbf{c}_i for its prediction $\tilde{\mathbf{a}}_i$ as:

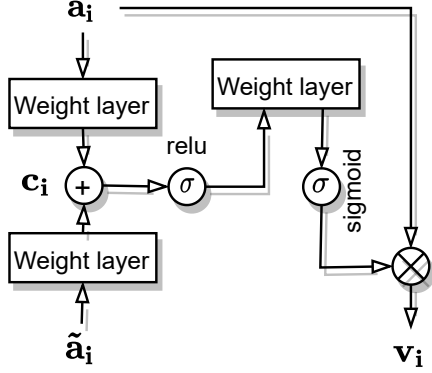
$$\mathbf{v}_i = \mathbf{a}_i * \sigma(W_{c_i} + \underbrace{\text{ReLU}(W_{a_i} \mathbf{a}_i + W_{\tilde{a}_i} \tilde{\mathbf{a}}_i + b_i)}_{\mathbf{c}_i}) \quad (11)$$

where σ is the sigmoid activation function, $W_* \in \mathbb{R}^{m \times m}$ and $b_i \in \mathbb{R}^{m \times 1}$ are trainable parameters. The resulting learned parameter \mathbf{c}_i is element-wise multiplied with the attribute detection scores \mathbf{a}_i to produce \mathbf{v}_i . The above operation constitutes the Attribute Re-weighting Layer (ARL). We implement the attribute layers as cascade of ARL layers. Finally, \mathbf{v}_i is concatenated with the global image representation for further classification. Figure 6a illustrates the ARL operation and Figure 6b shows how ARL is integrated into the attribute layers.

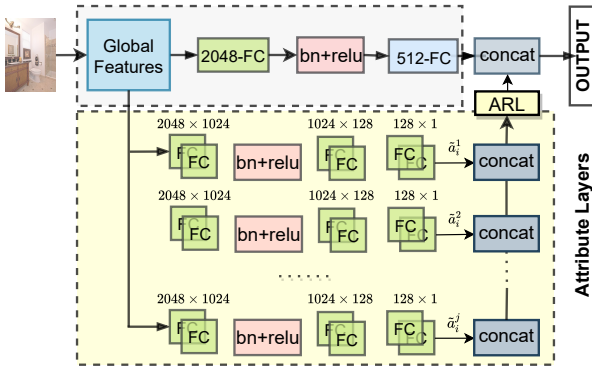
In summary, the motivation of designing the attribute re-weighting layer lies in two aspects. Firstly, by aggregating different kinds of attribute information to form a mid-level human semantic feature, we want to simulate the recognition process of human beings to form a compact attribute descriptor. Secondly, the detected object from object detection models can serve as a guidance for the global feature refinement process, promoting the performance of the recognition task.

V. EXPERIMENTS

We evaluate our model on four widely used scene datasets including ADE20K [5], MIT67 [16], SUN397 [6], and Places365 [17]. We use models pre-trained on COCO Object and COCO Panoptic datasets to predict objects (i.e., *things*) and concepts (i.e., *stuff*) for every scene datasets. The resulting



(a) The attribute re-weighting layer (ARL) is applied to the concatenated predictions obtained from each predictions before the sigmoid activation.



(b) The attribute prediction comprises j multidirectional branches and output $f(a_i^j)a_i^j \in \{a_i^1, a_i^2, \dots, a_i^j\}$ and f a multi-layer perceptron (MLP).

Fig. 6: The ARL and attribute layers built a cascade of MLP. For each attribute a_i^j of x_i , we predict a binary classification.

object predictions include all the 80 objects from the COCO datasets and all the 91 categories from the COCO Panoptic dataset with no overlaps. The final loss is then written as:

$$\mathcal{L}_{MASR} = \mathcal{L}_{att} + \mathcal{L}_{cls} \quad (12)$$

A. Datasets

ADE20K [5] is a scene parsing dataset exhaustively annotated with objects. The dataset contains 20,210 images for training, 2,000 images for testing, 3,000 images for validation and 1,055 categories.

MIT67 [16] is a challenging indoor scene dataset containing 67 categories and 15,620 images. 80 and 20 images per category are used for training and testing, respectively.

SUN397 [6] is a large-scale dataset containing 397 scene categories and 108,754 images. It contains 50 training images and 50 testing images per category.

Places-365 dataset is the subset of the original Places database [17] which includes over 7 million labeled pictures. The subset Places-365 contains 1,803,406 training images and 365 categories. The validation set contains 50 images per category and the test set contains 900 images per category.

B. Implementation details

In this section, we present the implementation details of our experiments. We use ResNet CNN models as backbones [44] pre-trained on ImageNet [45]. We add two fully connected layers $L^{K|}$ and $L^{A|}$ that projects 2048-dimensional vectors into the category and attribute spaces, respectively. All the images are resized into a resolution of 256×256 . We first train our network on the scene dataset alone (\mathcal{X}_I) for an initial 15 epochs in order to establish a basic feature representation. We then switch to the MASR setup and continue training for 85 epochs using Equation 12 loss. Our initial learning rate is set to 0.01 for the classifier parameters and to 0.001 for the base parameters and reduces by a factor of 0.1 every 20 epochs. We use a batchsize of 128 and stochastic gradient descent optimizer. We set the threshold ξ (see Eq. 3 and 9) to 80% and the minimum frequency β to 20.

C. Comparison with the baselines

Results on two datasets are shown in Table IV. We observed that the classification baseline yields a reasonable performance by achieving a top@1 accuracy of 79.3%, 70.8% and 54.7% on MIT67, SUN397 and ADE20K datasets respectively. We note that, for all the datasets, changing the backbone configurations from VGG to ResNet boost the performance accuracy by a factor of 7.7% on MIT67 dataset. Compared with the baselines, the use of attribute information alone (MASR w/o ARL) can improve the resulting top@1 performance by 4.1% on MIT67, 2% on SUN397, and 5.9% on ADE20K datasets. Compared with the proposed framework, we boost the baseline performance by factor of 6% – 10% on all the datasets.

D. Ablation studies

We further investigate the discriminative ability of our framework by visualizing the learned embedding and analyzing the effectiveness of the ARL as follows:

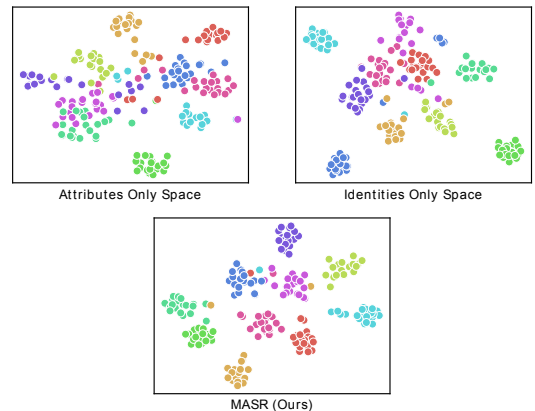


Fig. 7: Feature distributions of 10 random categories in the three feature spaces. Images are from MIT67 and different colors represent different categories.

TABLE IV: Ablation results for different backbone architectures. Classification accuracy on MIT67 with resnet101. Top k-accuracy and recall are shown. MASR (w/o ARL) denotes MASR without the attribute re-weighting layer

Models	MIT67			SUN397			ADE20K		
	Top@1	Top@2	Top@5	Top@1	Top@2	Top@5	Top@1	Top@2	Top@5
Baseline 1-VGG	71.6	83.1	91.7	46.5	60.0	73.4	44.6	53.7	62.6
Baseline 1-DenseNet161	74.0	84.9	92.5	58.4	72.7	85.7	55.2	66.2	77.4
Baseline 1-ResNet50	78.6	88.3	94.9	69.6	73.5	86.5	51.2	61.8	71.9
Baseline 1-ResNext101	82.3	90.3	96.0	70.8	83.1	91.4	54.7	65.6	74.8
MASR-VGG (w/o ARL)	75.2	86.9	93.7	56.8	71.0	84.8	54.3	66.6	76.9
MASR-ResNet50 (w/o ARL)	85.4	94.3	97.7	70.0	73.9	86.5	56.7	67.4	78.2
MASR-ResNext101 (w/o ARL)	86.4	93.3	98.2	72.8	84.4	93.1	60.6	70.0	79.7
MASR-VGG	76.9	88.0	94.6	60.1	75.2	86.7	61.3	72.5	80.4
MASR-ResNet50	86.2	94.8	98.9	73.2	78.1	89.3	62.7	74.1	82.9
MASR-ResNext101	88.5	95.3	98.7	75.01	86.8	94.6	64.4	75.2	85.1

TABLE V: Recognition accuracy comparison of some representative works on MIT67 dataset.

Traditional methods	Venue	Accuracy (%)
ROI [16]	CVPR'09	26.05
CENTRIST [21]	TPAMI'11	36.90
Hybrid parts [46]	ECCV'12	39.80
BOP [47]	CVPR'13	46.10
GI ST + SP [46]	ECCV'12	47.20
ISPR [48]	CVPR'14	50.10
Co-segmentation [49]	ICCV'13	51.40
DSFL [50]	ECCV'14	52.24
IFV [47]	CVPR'13	60.77
IFV + BOP [47]	CVPR'13	63.10
ISPR + IFV [48]	CVPR'14	68.50
CNN-based methods	Venue	Accuracy (%)
MOP-CNN [24]	ECCV'14	68.90
HybridNet [2]	NIPS'14	70.80
DSFL + CNN [50]	ECCV'14	76.23
DAG-CNN [25]	ICCV'15	77.50
Mix-CNN [23]	TOMM'19	79.63
CS(VGG-19) [13]	TCSVT'17	82.24
LS-DHM [25]	ICCV'15	83.75
Multi-scale CNNs [27]	CVPR'16	86.04
Dual CNN-DL [28]	AAAI'18	86.43
Multi-Resolution[51]	TIP'17	86.7
SDO [26]	PR'18	86.76
SemanticAware [3]	PR'20	87.10
MASR (Ours)		88.50

1) *Feature visualization*: To understand the learned feature representation, we randomly selected 10 categories from the test set and extracted their feature maps. We used t-SNE to visualize the embeddings by plotting their 2-dimension feature representation in Figure 7. Each point represents one image and points with the same color indicate image with the same category. In the attribute space, we see a somehow gathering of images with the same category while in the identity space, we observe a clear and constantly gathering of the images with the same color, which indicates that the model has learned a more discriminative feature representation. Compared to MARS feature space, the random selected categories are much more separated. We can see how images with the same color stay closer and far away from other color points. Only fewer

TABLE VI: Comparison of our proposed approach with other methods on SUN397 dataset.

Traditional Methods	Venue	Accuracy (%)
Semantic Manifold [52]	ECCV'12	28.90
OTC [22]	ECCV'14	34.56
cBoW + semantic [53]	IJCV'12	35.60
Xiao et al [6]	CVPR'10	38.00
FV (SIFT + LCS) [54]	IJCV'13	47.20
OTC + HOG2 \times 2 [22]	ECCV'14	49.60
CNN-based methods	Venue	Accuracy (%)
DeCAF [12]	ICML'14	40.94
MOP-CNN [24]	ECCV'14	51.98
HybridNet [2]	NIPS'14	53.86
Places-CNN [2]	NIPS'14	54.23
Places-CNN ft [2]	NIPS'14	56.20
DAG-CNN [25]	ICCV'15	56.20
Mix-CNN [23]	TOMM'19	57.47
CS(VGG-19) [13]	TCSVT'17	64.53
LS-DHM [25]	ICCV'15	67.56
Dual CNN-DL [28]	AAAI'18	70.13
Multi-scale CNNs [27]	CVPR'16	70.17
Multi-Resolution[51]	TIP'17	72.0
SDO [26]	PR'18	73.41
SemanticAware [3]	PR'20	74.04
MASR (Ours)		75.01

TABLE VII: Comparison results with other scene recognition methods on Places-365.

CNN-based methods	Venue	Accuracy (%)
Places365-ResNet [17]	TPAMI'18	54.74
Places356-VGG [17]	TPAMI'18	55.24
DenseNet-161 [3]	PR'20	56.12
Semantic Aware [3]	PR'20	56.51
CNN-SMN [55]	TIP'17	57.1
Fusing [56]	TCSVT'18	57.27
Multi-Resolution[51]	TIP'17	58.3
MASR (Ours)		56.61

different points are mixed. As a result, combing attributes with a re-weighting strategy helps to learn good representation and can achieve a better performance.

2) *The effectiveness of the attribute re-weighting layer*: To investigate the discriminative ability of the re-weighting

TABLE VIII: Comparison of scene recognition results on ADE20K dataset.

Methods	Venue	Accuracy (%)
ADE20k [5]	CVPR'17	45.38
Semantic Aware [3]	PR'20	62.55
MASR (Ours)		64.42

layer, we preform further experiments using MASR without ARL (MASR w/o ARL) and report the results on Tables IV. MASR (w/o ARL) is the network architecture where object attribute recognition task is simultaneously optimized with scene recognition task using Equations 9 and 12. We activate the attribute loss contribution to the overall task only after the 15th epoch. In general, we observe an increase in performance when adding attribute information to the Baseline 1 model. For example, in MIT67 dataset, MASR (w/o ARL) achieves a top@1 accuracy of 86.4% and outperforms Baseline 1 by a factor of 4.1%. Similarly, MASR, outperforms both MASR (w/o ARL) and Baseline 1 by a factor of 2.1% and 6.2% respectively. The performance improvement using ARL is consistent for all the datasets as shown in Table IV. This demonstrates that the features of jointly optimizing attribute and category losses are consistently much better when attribute are re-weighted by their scores. Finding the right weight also enable MASR to achieve a more discriminative feature representation.

E. Comparison with the state-of-the-art methods

We compare MASR to a number of recent approaches and report the results on Tables V, VI, VII, VIII. In general, we outperform most of the recent works, including Semantic Aware [3], and achieve competitive results with CNN-SMN [55], Fusing [56] and Multi-Resolution[51].

Evaluation on MIT67 dataset. Table V shows the evaluation results. We achieved an accuracy of 88.50% and improved the baseline top@1 accuracy by a factor of +6.2% (from 82.3% to 88.5%). Our method largely outperforms traditional methods. For instance, we surpass ISPR + IFV [48] by 20%. In general, traditional methods based on descriptor such as GIST [18] tends to perform poorly as they lack local structural information of a scene which is detrimental to the task.

Evaluation on SUN397 dataset. As shown in Table VI, we achieved an accuracy of 75.01%. Similar to the evaluation on MIT67 dataset, we surpass the traditional methods by a large margin. We exceed OTC + HOG2 \times 2 [22] by 25.41% and we gain a top@1 accuracy of 4.21% over the baseline. Moreover, our results on this dataset surpasses Semantic Aware [3] and Multi-Resolution [51] by 0.97% and 3.01%.

Evaluation on Places-365 dataset. The results on Table VII shows that Places-365 is a challenging dataset. At it's the most diverse and largest dataset. Recent works such as CNN-SMN [55] and Fusing [56] which achieved a top@1 accuracy of 57.1% and 57.27%, surpassed our model by small factors of 0.49% and 0.66%, respectively. In addition, Multi-Resolution [51], which exploits knowledge computed on validation data outperforms our model by 1.69%. We note

that Places-365 contains more than a million images and spans diverse scenes where common objects occur several times within the scene category with similar probability. Some discriminative parts of objets also appear with different shape and illumination. Consequently, the attribute objects obtained from this dataset by our technique is uniformly distributed across the scene categories. Our proposed technique may fail to take full advantage of the detected object scores. On small datasets, our technique performs well and can capture the discriminative object with high probabilities as shown on Table IV. Nonetheless, we have achieved competitive results with other models and surpassed SemanticAware[3].

Evaluation on ADE20K dataset. On this dataset, not many results are reported as illustrated in Table VIII. Yet, our method attains an accuracy of 64.42% exceeding SemanticAware [3] by 1.87%. We also improved the baseline performance from 54.7% to 64.4% and particularly outperformed the initial scene parsing model [5] on ADE20K datasets by 19.04%.

F. Evaluation of attribute recognition task

In this work, we developed a scene recognition approach which leverages information contained in automatically detected attributes to improve its classification results. However, we believe that these detected attributes can also be used for attribute recognition task. We test attribute recognition on MIT67 and SUN397 datasets and report the attribute detection score in Tables IX, X. We use the Baseline 2, trained specifically for the attribute recognition task (See Eq. 7). The Baseline 2 predicts a set of attribute given a scene image. We compute the precision as the ratio $\frac{TP}{TP+FP}$ where TP is the number of true positives and FP the number of false positives. By comparing the results of MASR and Baseline 2, we can draw two conclusions: First, on all datasets, the overall attribute recognition accuracy is improved by the proposed MASR network to some extent. The improvements are 1.1% and 0.08% on MIT67 and SUN397 respectively. In a nutshell, the integration of classification introduces some degree of complementary information and helps in learning a more discriminative attribute recognition model. Secondly, we observe that the recognition rate of some attributes decreases for MASR, such as “person”, “floor”, and “ceiling” in MIT67 dataset. This can be explained by the fact that MIT67 is an indoor dataset. As a results, attributes such as “floor”, “ceiling”, span several scene categories, and are present with a high probability across various different categories. Moreover, the reason probably lies in the multi-task nature of MASR. The model is primarily optimized for classification while attribute recognition task is a multi-label classification problem. Moreover, ambiguous images of certain attributes may be incorrectly predicted by the object detection model. Nevertheless, the improvement on the two datasets is still encouraging and further investigations should be critical.

VI. CONCLUSION AND FUTURE WORK

In this paper, we proposed a Multi-task Attribute-scene recognition (MASR) network that exploits both category labels and attribute annotations. By combining the two tasks, the

TABLE IX: Attribute recognition accuracy on MIT67. We only show 10 attribute objects. AP stands for Average Precision. B2 denotes 'Baseline 2'.

	person	counter	floor	shelf	window	ceiling	cabinet	table	building	rug	AP
B2	75.5	89.3	77.7	77.4	76.2	91.5	72.0	76.7	84.0	81.4	86.0
MASR	72.7	100.0	73.0	77.0	90.2	88.9	89.6	100.0	87.5	80.0	87.1

TABLE X: Attribute recognition accuracy on SUN397. We also report the 10 most occurring attributes. PAV: pavement, AP: average precision, MOU: mountain, BUI: building, CA: cabinet, WI: Windows, CE: ceiling. B2 denotes 'Baseline 2'.

	person	river	sea	shelf	WI	tree	CE	CA	PAV	MOU	grass	dirt	BUI	AP
B2	71.6	97.7	98.2	89.5	75.8	93.2	90.9	97.0	74.9	92.2	90.3	87.8	84.7	88.1
MASR	77.4	93.9	93.0	82.6	79.7	92.5	87.1	92.5	76.2	88.0	89.3	88.3	83.0	89.7

MASR network is able to learn more discriminative feature representations for scene, including attribute features and scene features. Specifically, we mined attribute labels from existing object-centric datasets and considered their predictions as additional cues for scene classification. Extensive experiment on four large-scale datasets showed that our method achieves competitive recognition accuracy compared to the state-of-the-art methods. We also showed that the proposed MASR yields improvement in the attribute recognition task over the baseline in all the testing datasets.

In future work, we will investigate the transferability and scalability of scene attributes. For example, we could adapt the attribute model learned on SUN397 dataset to other scene datasets. Secondly, attributes provide a bridge to the image-text understanding. We could investigate a system using attributes to retrieve the relevant scene images. It is useful in solving specific image retrieval problems, in which the query image is missing and can be described by attributes.

REFERENCES

- [1] M. Cordts, M. Omran, S. Ramos, T. Rehfeld, M. Enzweiler, R. Benenson, U. Franke, S. Roth, and B. Schiele, "The cityscapes dataset for semantic urban scene understanding," in *2016 IEEE CVPR*, 2016, pp. 3213–3223.
- [2] B. Zhou, A. Lapedriza, J. Xiao, A. Torralba, and A. Oliva, "Learning deep features for scene recognition using places database," in *Proceedings of the 27th NIPS - Volume 1*, ser. NIPS'14. Cambridge, MA, USA: MIT Press, 2014, p. 487–495.
- [3] A. López-Cifuentes, M. Escudero-Viñolo, J. Bescós, and Álvaro García-Martín, "Semantic-aware scene recognition," *Pattern Recognition*, vol. 102, p. 107256, 2020.
- [4] Y. Wu, A. Kirillov, F. Massa, W.-Y. Lo, and R. Girshick, "Detectron2," <https://github.com/facebookresearch/detectron2>, 2019.
- [5] B. Zhou, H. Zhao, X. Puig, S. Fidler, A. Barriuso, and A. Torralba, "Scene parsing through ade20k dataset," in *2017 IEEE Conference on Computer Vision and Pattern Recognition (CVPR)*, 2017, pp. 5122–5130.
- [6] J. Xiao, J. Hays, K. A. Ehinger, A. Oliva, and A. Torralba, "Sun database: Large-scale scene recognition from abbey to zoo," in *2010 IEEE Computer Society Conference on Computer Vision and Pattern Recognition*, 2010, pp. 3485–3492.
- [7] N. Dalal and B. Triggs, "Histograms of oriented gradients for human detection," in *2005 IEEE Computer Society Conference on Computer Vision and Pattern Recognition (CVPR'05)*, vol. 1, 2005, pp. 886–893 vol. 1.
- [8] D. G. Lowe, "Object recognition from local scale-invariant features," in *Proceedings of the Seventh IEEE International Conference on Computer Vision*, vol. 2, 1999, pp. 1150–1157 vol.2.
- [9] E. Shechtman and M. Irani, "Matching local self-similarities across images and videos," in *2007 IEEE Conference on Computer Vision and Pattern Recognition*, 2007, pp. 1–8.
- [10] X. Meng, Z. Wang, and L. Wu, "Building global image features for scene recognition," *Pattern Recognition*, vol. 45, no. 1, pp. 373 – 380, 2012.
- [11] M. Cimpoi, S. Maji, and A. Vedaldi, "Deep filter banks for texture recognition and segmentation," in *2015 IEEE Conference on Computer Vision and Pattern Recognition (CVPR)*, 2015, pp. 3828–3836.
- [12] J. Donahue, Y. Jia, O. Vinyals, J. Hoffman, N. Zhang, E. Tzeng, and T. Darrell, "Decaf: A deep convolutional activation feature for generic visual recognition," in *Proceedings of the 31st International Conference on Machine Learning - Volume 32*, ser. ICML'14. JMLR.org, 2014, p. 1–647–655.
- [13] G. Xie, X. Zhang, S. Yan, and C. Liu, "Hybrid cnn and dictionary-based models for scene recognition and domain adaptation," *IEEE Transactions on Circuits and Systems for Video Technology*, vol. 27, no. 6, pp. 1263–1274, 2017.
- [14] G. Chen, X. Song, H. Zeng, and S. Jiang, "Scene recognition with prototype-agnostic scene layout," *IEEE Transactions on Image Processing*, vol. 29, pp. 5877–5888, 2020.
- [15] A. R. Zamir, A. Sax, W. Shen, L. Guibas, J. Malik, and S. Savarese, "Taskonomy: Disentangling task transfer learning," in *2018 IEEE/CVF Conference on Computer Vision and Pattern Recognition*, 2018, pp. 3712–3722.
- [16] A. Quattoni and A. Torralba, "Recognizing indoor scenes," in *2009 IEEE Conference on Computer Vision and Pattern Recognition*, 2009, pp. 413–420.
- [17] B. Zhou, A. Lapedriza, A. Khosla, A. Oliva, and A. Torralba, "Places: A 10 million image database for scene recognition," *IEEE Transactions on Pattern Analysis and Machine Intelligence*, vol. 40, no. 6, pp. 1452–1464, 2018.
- [18] A. Oliva, "Chapter 41 - gist of the scene," in *Neurobiology of Attention*, L. Itti, G. Rees, and J. K. Tsotsos, Eds. Burlington: Academic Press, 2005, pp. 251 – 256.
- [19] S. Lazebnik, C. Schmid, and J. Ponce, "Beyond bags of features: Spatial pyramid matching for recognizing natural scene categories," in *2006 IEEE Computer Society Conference on Computer Vision and Pattern Recognition (CVPR'06)*, vol. 2, 2006, pp. 2169–2178.
- [20] J. Krapac, J. Verbeek, and F. Jurie, "Modeling spatial layout with fisher vectors for image categorization," in *2011 International Conference on Computer Vision*, 2011, pp. 1487–1494.
- [21] J. Wu and J. M. Rehg, "Centrist: A visual descriptor for scene categorization," *IEEE Transactions on Pattern Analysis and Machine Intelligence*, vol. 33, no. 8, pp. 1489–1501, 2011.
- [22] R. Margolin, L. Zelnik-Manor, and A. Tal, "Otc: A novel local descriptor for scene classification," in *Computer Vision – ECCV 2014*. Cham: Springer International Publishing, 2014, pp. 377–391.
- [23] S. Jiang, G. Chen, X. Song, and L. Liu, "Deep patch representations with shared codebook for scene classification," *ACM Trans. Multimedia Comput. Commun. Appl.*, vol. 15, no. 1s, Jan. 2019.
- [24] Y. Gong, L. Wang, R. Guo, and S. Lazebnik, "Multi-scale orderless pooling of deep convolutional activation features," in *Computer Vision – ECCV 2014*. Cham: Springer International Publishing, 2014, pp. 392–407.

- [25] S. Yang and D. Ramanan, "Multi-scale recognition with dag-cnns," in *2015 IEEE International Conference on Computer Vision (ICCV)*, 2015, pp. 1215–1223.
- [26] X. Cheng, J. Lu, J. Feng, B. Yuan, and J. Zhou, "Scene recognition with objectness," *Pattern Recognition*, vol. 74, pp. 474–487, 2018.
- [27] L. Herranz, S. Jiang, and X. Li, "Scene recognition with cnns: Objects, scales and dataset bias," in *2016 IEEE Conference on Computer Vision and Pattern Recognition (CVPR)*, 2016, pp. 571–579.
- [28] Y. Liu, Q. Chen, W. Chen, and I. Wassell, "Dictionary learning inspired deep network for scene recognition," 2018.
- [29] P. Li, X. Li, X. Li, H. Pan, M. Khyam, M. Noor-A-Rahim, and S. S. Ge, "Place perception from the fusion of different image representation," *Pattern Recognition*, vol. 110, p. 107680, 2021.
- [30] Y. Lin, L. Zheng, Z. Zheng, Y. Wu, Z. Hu, C. Yan, and Y. Yang, "Improving person re-identification by attribute and identity learning," *Pattern Recognition*, vol. 95, pp. 151–161, 2019.
- [31] C. Tay, S. Roy, and K. Yap, "Aanet: Attribute attention network for person re-identifications," in *2019 IEEE/CVF Conference on Computer Vision and Pattern Recognition (CVPR)*, 2019, pp. 7127–7136.
- [32] B. Yao, X. Jiang, A. Khosla, A. L. Lin, L. Guibas, and L. Fei-Fei, "Human action recognition by learning bases of action attributes and parts," in *2011 International Conference on Computer Vision*, 2011, pp. 1331–1338.
- [33] D. Roy, K. S. R. Murty, and C. K. Mohan, "Unsupervised universal attribute modeling for action recognition," *IEEE Transactions on Multimedia*, vol. 21, no. 7, pp. 1672–1680, 2019.
- [34] V. Ferrari and A. Zisserman, "Learning visual attributes," in *Proceedings of the 20th International Conference on Neural Information Processing Systems*, ser. NIPS'07. Red Hook, NY, USA: Curran Associates Inc., 2007, p. 433–440.
- [35] C. H. Lampert, H. Nickisch, and S. Harmeling, "Learning to detect unseen object classes by between-class attribute transfer," in *2009 IEEE Conference on Computer Vision and Pattern Recognition*, 2009, pp. 951–958.
- [36] H. Zeng, X. Song, G. Chen, and S. Jiang, "Learning scene attribute for scene recognition," *IEEE Transactions on Multimedia*, vol. 22, no. 6, pp. 1519–1530, 2020.
- [37] G. Patterson and J. Hays, "Sun attribute database: Discovering, annotating, and recognizing scene attributes," in *2012 IEEE Conference on Computer Vision and Pattern Recognition*, 2012, pp. 2751–2758.
- [38] F. M. Rueda and G. A. Fink, "Learning attribute representation for human activity recognition," in *2018 24th International Conference on Pattern Recognition (ICPR)*, 2018, pp. 523–528.
- [39] Y. Xian, C. H. Lampert, B. Schiele, and Z. Akata, "Zero-shot learning—a comprehensive evaluation of the good, the bad and the ugly," *IEEE Transactions on Pattern Analysis and Machine Intelligence*, vol. 41, no. 9, pp. 2251–2265, 2019.
- [40] A. Oliva and A. Torralba, "Modeling the shape of the scene: A holistic representation of the spatial envelope," *International Journal of Computer Vision*, vol. 42, no. 3, pp. 145–175, May 2001.
- [41] S. Wang, J. Joo, Y. Wang, and S. Zhu, "Weakly supervised learning for attribute localization in outdoor scenes," in *2013 IEEE Conference on Computer Vision and Pattern Recognition*, 2013, pp. 3111–3118.
- [42] W. Ouyang, H. Li, X. Zeng, and X. Wang, "Learning deep representation with large-scale attributes," in *2015 IEEE International Conference on Computer Vision (ICCV)*, 2015, pp. 1895–1903.
- [43] G. Patterson, C. Xu, H. Su, and J. Hays, "The sun attribute database: Beyond categories for deeper scene understanding," *International Journal of Computer Vision*, vol. 108, no. 1, p. 59, May 2014.
- [44] K. He, X. Zhang, S. Ren, and J. Sun, "Deep residual learning for image recognition," in *2016 IEEE Conference on Computer Vision and Pattern Recognition (CVPR)*, 2016, pp. 770–778.
- [45] J. Deng, W. Dong, R. Socher, L. Li, Kai Li, and Li Fei-Fei, "Imagenet: A large-scale hierarchical image database," in *2009 IEEE Conference on Computer Vision and Pattern Recognition*, 2009, pp. 248–255.
- [46] Y. Zheng, Y.-G. Jiang, and X. Xue, "Learning hybrid part filters for scene recognition," in *Computer Vision – ECCV 2012*. Berlin, Heidelberg: Springer Berlin Heidelberg, 2012, pp. 172–185.
- [47] M. Juneja, A. Vedaldi, C. V. Jawahar, and A. Zisserman, "Blocks that shout: Distinctive parts for scene classification," in *2013 IEEE Conference on Computer Vision and Pattern Recognition*, 2013, pp. 923–930.
- [48] D. Lin, C. Lu, R. Liao, and J. Jia, "Learning important spatial pooling regions for scene classification," in *2014 IEEE Conference on Computer Vision and Pattern Recognition*, 2014, pp. 3726–3733.
- [49] J. Sun and J. Ponce, "Learning discriminative part detectors for image classification and cosegmentation," in *2013 IEEE International Conference on Computer Vision*, 2013, pp. 3400–3407.
- [50] Z. Zuo, G. Wang, B. Shuai, L. Zhao, Q. Yang, and X. Jiang, "Learning discriminative and shareable features for scene classification," in *Computer Vision – ECCV 2014*. Cham: Springer International Publishing, 2014, pp. 552–568.
- [51] L. Wang, S. Guo, W. Huang, Y. Xiong, and Y. Qiao, "Knowledge guided disambiguation for large-scale scene classification with multi-resolution cnns," *IEEE Transactions on Image Processing*, vol. 26, no. 4, pp. 2055–2068, 2017.
- [52] R. Kwitt, N. Vasconcelos, and N. Rasiwasia, "Scene recognition on the semantic manifold," in *Computer Vision – ECCV 2012*. Berlin, Heidelberg: Springer Berlin Heidelberg, 2012, pp. 359–372.
- [53] Y. Su and F. Jurie, "Improving image classification using semantic attributes," *International Journal of Computer Vision*, vol. 100, no. 1, pp. 59–77, may 2012.
- [54] J. Sánchez, F. Perronnin, T. Mensink, and J. Verbeek, "Image classification with the fisher vector: Theory and practice," *International Journal of Computer Vision*, vol. 105, no. 3, pp. 222–245, jun 2013.
- [55] X. Song, S. Jiang, and L. Herranz, "Multi-scale multi-feature context modeling for scene recognition in the semantic manifold," *IEEE Transactions on Image Processing*, vol. 26, no. 6, pp. 2721–2735, 2017.
- [56] N. Sun, W. Li, J. Liu, G. Han, and C. Wu, "Fusing object semantics and deep appearance features for scene recognition," *IEEE Transactions on Circuits and Systems for Video Technology*, vol. 29, no. 6, pp. 1715–1728, 2019.